mitogen for mature hepatocytes and was cloned in 1989 (12, 13). In addition to its hepatotrophic effect, HGF was revealed to exhibit neurotrophic activity in the hippocampus, cerebral cortex, sensory neurons, and motor neurons (14, 20). Recently, Hayashi et al. (21) reported that *HGF* gene transfer to the subarachnoid space prevents delayed neuronal death in gerbil hippocampal CA1 neurons. Sun and Nakamura et al. (46) reported that introduction of the *HGF* gene into neurons of ALS-model mice attenuates motor-neuronal degeneration and increases the lifespan of these mice. We demonstrate here that human HGF was detected in both CSF and SGCs and that it induced the expression of rat endogenous HGF. Moreover, the induction of HGF increased expression of the HGF receptor c-Met in SGCs to augment signal transduction of HGF. HGF is also known to have anti-apoptotic activity by increasing the ratio of bcl-2 to bax through the PI3K/Akt pathway (47) and to have the capacity to induce angiogenesis and increase blood flow (48–51). These functions of HGF can be enhanced by a positive feedback mechanism. Recent studies have shown that the feedback mechanism involved in HGF signaling is mediated by an essential transcription factor, ets. Aoki et al. (48) demonstrated that HGF up-regulates ets activity and ets-1 protein. Not only rat HGF, but also exogenously expressed human HGF, stimulates endogenous HGF expression through the induction of ets activity (49). A RAS-RAF-MEK-ERK signaling pathway is involved in the activation of ets-1 transcription by HGF (52). When ets-1 expression was inhibited by the transfection of antisense ets-1 oligodeoxynucleotides, HGF expression was markedly decreased (49, 50). In this study, the biological effects of HGF appeared to be up-regulated multifold by such a positive feedback mechanism, although the level of human HGF in CSF was much lower than rat HGF after stimulation by human HGF. *HGF* gene therapy for the auditory system may have several advantages over the previous gene therapy strategies using neurotrophins, but further comparative experiments using other neurotrophins are needed. Although the precise measurement of cochlear blood flow would be difficult, further study of vascular function in the cochlea after HGF gene transfer will provide novel information regarding cochlear function. Moreover, there exists another possibility in which HGF could cause the regeneration of HC or SGC as implied in this study, and we are now investigating the regenerative effect of HGF on inner ear cells. Combined therapy of cochlear implant and HGF gene therapy, i.e., administering the *HGF* gene during the operation of cochlear implant, would be also effective.

Hearing impairment was associated with the loss of HC and SGC, and the prevention of their loss was achieved by the protective effect of HGF against apoptotic cell death. HGF expression was also effective for the recovery of hearing function, after previous impairment by kanamycin treatment. Thus, *HGF* gene therapy is a potent candidate for the treatment of sensorineural hearing impairment. This research provides a new insight and approach for clinical treatment for hearing impairment by combining the *HGF* gene with the HVJ-E vector delivery system.

ACKNOWLEDGMENTS

We thank Yoshinaga Saeki, Masayuki Endoh, Seiji Yamamoto, Yo C.Y., and members of our laboratory for helpful comments and discussions. This work was supported by grants from the Ministry of Health, Labor and Welfare of Japan.

REFERENCES

1. Mills, J. H., and Going, J. A. (1982) Review of environmental factors affecting hearing. *Environ. Health Perspect.* **44**, 119–127

2. Spoendlin, H. (1975) Retrograde degeneration of the cochlear nerve. *Acta Otolaryngol.* **79,** 266–275

3. Bichler, E., Spoendlin, H., and Rauchegger, H. (1983) Degeneration of cochlear neurons after amikacin intoxication in the rat. *Arch. Otorhinolaryngol.* **237,** 201–208

4. Incesulu, A., and Nadol, J. B., Jr. (1998) Correlation of acoustic threshold measures and spiral ganglion cell survival in severe to profound sensorineural hearing loss: implications for cochlear implantation. *Ann. Otol. Rhinol. Laryngol.* **107,** 906–911

5. Bowers, W. J., Chen, X., Guo, H., Frisina, D. R., Federoff, H. J., and Frisina, R. D. (2002) Neurotrophin-3 transduction attenuates Cisplatin spiral ganglion neuron ototoxicity in the cochlea. *Mol. Ther.* **6,** 12–18

6. Chen, X., Frisina, R. D., Bowers, W. J., Frisina, D. R., and Federoff, H. J. (2001) HSV amplicon-mediated neurotrophin-3 expression protects murine spiral ganglion neurons from cisplatin-induced damage. *Mol. Ther.* **3,** 958–963

7. Ernfors, P., Duan, M. L., ElShamy, W. M., and Canlon, B. (1996) Protection of auditory neurons from aminoglycoside toxicity by neurotrophin-3. *Nat. Med.* **2,** 463–467

8. Gabaizadeh, R., Staecker, H., Liu, W., Kopke, R., Malgrange, B., Lefebvre, P. P., and Van de Water, T. R. (1997) Protection of both auditory hair cells and auditory neurons from cisplatin induced damage. *Acta Otolaryngol.* **117,** 232–238

9. Gao, W. Q. (1998) Therapeutic potential of neurotrophins for treatment of hearing loss. *Mol. Neurobiol.* **17,** 17–31

10. Staecker, H., Kopke, R., Malgrange, B., Lefebvre, P., and Van de Water, T. R. (1996) NT-3 and/or BDNF therapy prevents loss of auditory neurons following loss of hair cells. *Neuroreport* **7,** 889–894

11. Yagi, M., Kanzaki, S., Kawamoto, K., Shin, B., Shah, P. P., Magal, E., Sheng, J., and Raphael, Y. (2000) Spiral ganglion neurons are protected from degeneration by GDNF gene therapy. *J. Assoc. Res. Otolaryngol.* **1,** 315–325

12. Nakamura, T., Nawa, K., and Ichihara, A. (1984) Partial purification and characterization of hepatocyte growth factor from serum of hepatectomized rats. *Biochem. Biophys. Res. Commun.* **122,** 1450–1459

13. Nakamura, T., Nishizawa, T., Hagiya, M., Seki, T., Shimonishi, M., Sugimura, A., Tashiro, K., and Shimizu, S. (1989) Molecular cloning and expression of human hepatocyte growth factor. *Nature* **342,** 440–443

14. Honda, S., Kagoshima, M., Wanaka, A., Tohyama, M., Matsumoto, K., and Nakamura, T. (1995) Localization and functional coupling of HGF and c-Met/HGF receptor in rat brain: implication as neurotrophic factor. *Brain Res. Mol. Brain Res.* **32,** 197–210

15. Sun, W., Funakoshi, H., and Nakamura, T. (2002) Localization and functional role of hepatocyte growth factor (HGF) and its receptor c-met in the rat developing cerebral cortex. *Brain Res. Mol. Brain Res.* **103,** 36–48

16. Hashimoto, N., Yamanaka, H., Fukuoka, T., Dai, Y., Obata, K., Mashimo, T., and Noguchi, K. (2001) Expression of HGF and cMet in the peripheral nervous system of adult rats following sciatic nerve injury. *Neuroreport* **12,** 1403–1407

17. Hashimoto, N., Yamanaka, H., Fukuoka, T., Obata, K., Mashimo, T., and Noguchi, K. (2001) Expression of hepatocyte growth factor in primary sensory neurons of adult rats. *Brain Res. Mol. Brain Res.* **97,** 83–88

18. Jung, W., Castren, E., Odenthal, M., Vande Woude, G. F., Ishii, T., Dienes, H. P., Lindholm, D., and Schirmacher, P. (1994) Expression and functional interaction of hepatocyte growth factor-scatter factor and its receptor c-met in mammalian brain. *J. Cell Biol.* **126,** 485–494

19. Maina, F., Hilton, M. C., Ponzetto, C., Davies, A. M., and Klein, R. (1997) Met receptor signaling is required for sensory nerve development and HGF promotes axonal growth and survival of sensory neurons. *Genes Dev.* **11,** 3341–3350

20. Maina, F., and Klein, R. (1999) Hepatocyte growth factor, a versatile signal for developing neurons. *Nat. Neurosci.* **2,** 213–217

21. Hayashi, K., Morishita, R., Nakagami, H., Yoshimura, S., Hara, A., Matsumoto, K., Nakamura, T., Ogihara, T., Kaneda, Y., and Sakai, N. (2001) Gene therapy for preventing neuronal death using hepatocyte growth factor: in vivo gene transfer of HGF to subarachnoid space prevents delayed neuronal death in gerbil hippocampal CA1 neurons. *Gene Ther.* **8,** 1167–1173

22. Miyazawa, T., Matsumoto, K., Ohmichi, H., Katoh, H., Yamashima, T., and Nakamura, T. (1998) Protection of hippocampal neurons from ischemia-induced delayed neuronal death by hepatocyte growth factor: a novel neurotrophic factor. *J. Cereb. Blood Flow Metab.* **18,** 345–348

23. Yamada, K., Moriguchi, A., Morishita, R., Aoki, M., Nakamura, Y., Mikami, H., Oshima, T., Ninomiya, M., Kaneda, Y., Higaki, J., et al. (1996) Efficient oligonucleotide delivery using the HVJ-liposome method in the central nervous system. *Am. J. Physiol.* **271,** R1212–R1220

24. Yoshimura, S., Morishita, R., Hayashi, K., Kokuzawa, J., Aoki, M., Matsumoto, K., Nakamura, T., Ogihara, T., Sakai, N., and Kaneda, Y. (2002) Gene transfer of hepatocyte growth factor to subarachnoid space in cerebral hypoperfusion model. *Hypertension* **39,** 1028–1034

25. Doi, K., Hasagawa, T., Fuse, Y., Uno, Y., Fujii, K., and Kubo, T. (1999) Change of auditory system in animal model of cochlear implant. *Otol. Jpn* **9,** 85–90

26. Wu, W. J., Sha, S. H., McLaren, J. D., Kawamoto, K., Raphael, Y., and Schacht, J. (2001) Aminoglycoside ototoxicity in adult CBA, C57BL and BALB mice and the Sprague-Dawley rat. *Hear. Res.* **158,** 165–178

27. Forge, A., and Schacht, J. (2000) Aminoglycoside antibiotics. *Audiol. Neurootol.* **5,** 3–22

28. Kaneda, Y., Nakajima, T., Nishikawa, T., Yamamoto, S., Ikegami, H., Suzuki, N., Nakamura, H., Morishita, R., and Kotani, H. (2002) Hemagglutinating virus of Japan (HVJ) envelope vector as a versatile gene delivery system. *Mol. Ther.* **6,** 219

29. Shimamura, M., Morishita, R., Endoh, M., Oshima, K., Aoki, M., Waguri, S., Uchiyama, Y., and Kaneda, Y. (2003) HVJ-envelope vector for gene transfer into central nervous system. *Biochem. Biophys. Res. Commun.* **300,** 464–471

30. Tomita, N., Morishita, R., Higaki, J., Tomita, S., Aoki, M., Kaneda, Y., and Ogihara, T. (1996) Sustained transgene expression by transfection of renin gene into liver of neonates. *Biochem. Biophys. Res. Commun.* **224,** 43–49

31. Tsujie, M., Isaka, Y., Nakamura, H., Imai, E., and Hori, M. (2001) Electroporation-mediated gene transfer that targets glomeruli. *J. Am. Soc. Nephrol.* **12,** 949–954

32. Sun, W., Funakoshi, H., and Nakamura, T. (1999) Differential expression of hepatocyte growth factor and its receptor, c-Met in the rat retina during development. *Brain Res.* **851,** 46–53

33. Ueki, T., Kaneda, Y., Tsutsui, H., Nakanishi, K., Sawa, Y., Morishita, R., Matsumoto, K., Nakamura, T., Takahashi, H., Okamoto, E., et al. (1999) Hepatocyte growth factor gene therapy of liver cirrhosis in rats. *Nat. Med.* **5,** 226–230

34. Tsao, M. S., Zhu, H., Giaid, A., Viallet, J., Nakamura, T., and Park, M. (1993) Hepatocyte growth factor/scatter factor is an autocrine factor for human normal bronchial epithelial and lung carcinoma cells.PG - 571-9. *Cell Growth Differ.* **4,** 571–579

35. Yang, X. M., Toma, J. G., Bamji, S. X., Belliveau, D. J., Kohn, J., Park, M., and Miller, F. D. (1998) Autocrine hepatocyte growth factor provides a local mechanism for promoting axonal growth. *J. Neurosci.* **18,** 8369–8381

36. Kawamoto, K., Oh, S. H., Kanzaki, S., Brown, N., and Raphael, Y. (2001) The functional and structural outcome of inner ear gene transfer via the vestibular and cochlear fluids in mice. *Mol. Ther.* **4,** 575–585

37. Stöver, T., Yagi, M., and Raphael, Y. (1999) Cochlear gene transfer: round window versus cochleostomy inoculation. *Hear. Res.* **136,** 124–130

38. Jero, J., Mhatre, A. N., Tseng, C. J., Stern, R. E., Coling, D. E., Goldstein, J. A., Hong, K., Zheng, W. W., Hoque, A. T., and Lalwani, A. K. (2001) Cochlear gene delivery through an intact round window membrane in mouse. *Hum. Gene Ther.* **12,** 539–548

39. Yamasoba, T., Yagi, M., Roessler, B. J., Miller, J. M., and Raphael, Y. (1999) Inner ear transgene expression after adenoviral vector inoculation in the endolymphatic sac. *Hum. Gene Ther.* **10,** 769–774

40. Lalwani, A. K., Han, J. J., Walsh, B. J., Zolotukhin, S., Muzyczka, N., and Mhatre, A. N. (1997) Green fluorescent protein as a reporter for gene transfer studies in the cochlea. *Hear. Res.* **114,** 139–147

41. Kho, S. T., Pettis, R. M., Mhatre, A. N., and Lalwani, A. K. (2000) Safety of adeno-associated virus as cochlear gene transfer vector: analysis of distant spread beyond injected cochleae. *Mol. Ther.* **2,** 368–373

42. Stover, T., Yagi, M., and Raphael, Y. (2000) Transduction of the contralateral ear after adenovirus-mediated cochlear gene transfer. *Gene Ther.* **7,** 377–383

43. Kaneda, Y., Iwai, K., and Uchida, T. (1989) Increased expression of DNA cointroduced with nuclear protein in adult rat liver. *Science* **243,** 375–378

44. Kaneda, Y., Saeki, Y., and Morishita, R. (1999) Gene therapy using HVJ-liposomes: the best of both worlds? *Mol. Med. Today* **5,** 298–303

45. Kato, K., Nakanishi, M., Kaneda, Y., Uchida, T., and Okada, Y. (1991) Expression of hepatitis B virus surface antigen in adult rat liver. Co-introduction of DNA and nuclear protein by a simplified liposome method. *J. Biol. Chem.* **266,** 3361–3364

46. Sun, W., Funakoshi, H., and Nakamura, T. (2002) Overexpression of HGF retards disease progression and prolongs life span in a transgenic mouse model of ALS. *J. Neurosci.* **22,** 6537–6548

47. Nakagami, H., Morishita, R., Yamamoto, K., Taniyama, Y., Aoki, M., Yamasaki, K., Matsumoto, K., Nakamura, T., Kaneda, Y., and Ogihara, T. (2002) Hepatocyte growth factor prevents endothelial cell death through inhibition of bax translocation from cytosol to mitochondrial membrane. *Diabetes* **51,** 2604–2611

48. Aoki, M., Morishita, R., Taniyama, Y., Kida, I., Moriguchi, A., Matsumoto, K., Nakamura, T., Kaneda, Y., Higaki, J., and Ogihara, T. (2000) Angiogenesis induced by hepatocyte growth factor in non-infarcted myocardium and infarcted myocardium: up-regulation of essential transcription factor for angiogenesis, ets. *Gene Ther.* **7,** 417–427

49. Morishita, R. (2002) Recent progress in gene therapy for cardiovascular disease. *Circ. J.* **66,** 1077–1086

50. Tomita, N., Morishita, R., Taniyama, Y., Koike, H., Aoki, M., Shimizu, H., Matsumoto, K., Nakamura, T., Kaneda, Y., and Ogihara, T. (2003) Angiogenic property of hepatocyte growth factor is dependent on upregulation of essential transcription factor for angiogenesis, ets-1. *Circulation* **107,** 1411–1417

51. Taniyama, Y., Morishita, R., Aoki, M., Hiraoka, K., Yamasaki, K., Hashiya, N., Matsumoto, K., Nakamura, T., Kaneda, Y., and Ogihara, T. (2002) Angiogenesis and antifibrotic action by hepatocyte growth factor in cardiomyopathy. *Hypertension* **40,** 47–53

52. Paumelle, R., Tulasne, D., Kherrouche, Z., Plaza, S., Leroy, C., Reveneau, S., Vandenbunder, B., Fafeur, V., Tulashe, D., and Reveneau, S. (2002) Hepatocyte growth factor/scatter factor activates the ETS1 transcription factor by a RAS-RAF-MEK-ERK signaling pathway. *Oncogene* **21,** 2309–2319

Received July 18, 2003; accepted October 1, 2003.

Table 1

Luciferase activity at 24 h after transfection of *HGF* gene via the cisterna magna

	RLU/mg tissue
Cerebral cortex	151.2 ± 224.7 (n=4)
Medulla	225.3 ± 88.2 (n=4)
Cerebellum	112.3 ± 61.4 (n=4)
Cochlea	146.6 ± 44.7 (n=8)

After intrathecal injection of the luciferase gene via the cisterna magna, luciferase activity was measured from tissues dissected from the cerebral cortex, medulla, cerebellum, and cochlear. Transgene expression was not detected in other organs including the liver, lung, and spleen.

Fig. 1

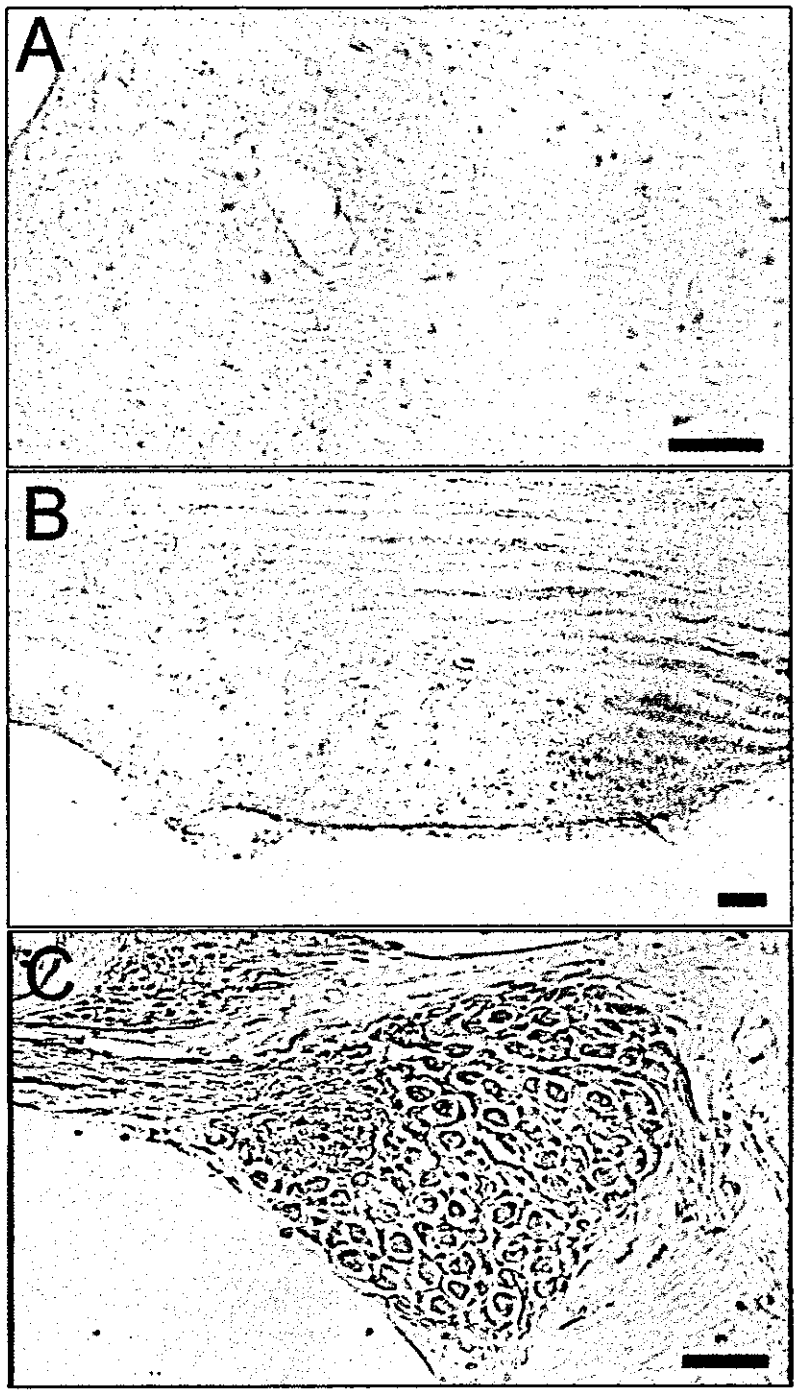

Figure 1. Localization of *lacZ* expression in the brain and cochlea. *lacZ* expression in the medulla (*A*), cochlear nucleus (*B*), and SGCs (*C*) of normal rats was detected by X-gal staining on day 7 after intrathecal injection of HVJ-E containing the *E. coli* β-galactosidase gene *lacZ*. Scale bar: 100μm.

Fig. 2

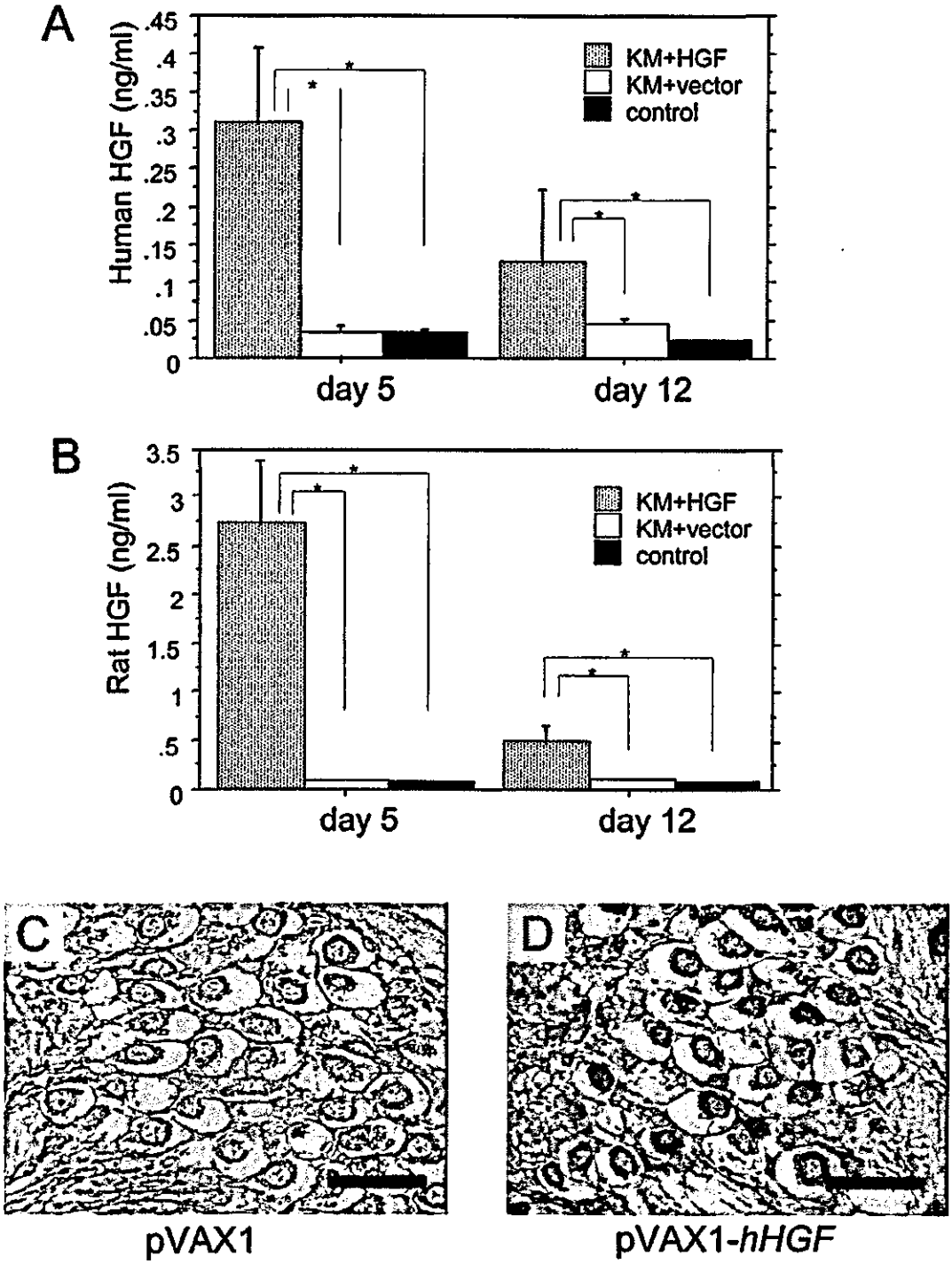

Figure 2. Expression levels of exogenous and endogenous HGF in CSF and SGCs. Exogenous human HGF (*A*) and endogenous rat HGF (*B*) in CSF from the KM + HGF, KM + vector, and control groups were measured on days 5 and 12 after transfection with the human HGF transgene (n=4 for each). SGCs from the mid-turn of cochleae treated with KM + vector (*C*) or KM + HGF (*D*) were immunostained with anti-human HGF antibody. *$P < 0.01$. Scale bar: 50 μm; n=4 for each group.

Fig. 3

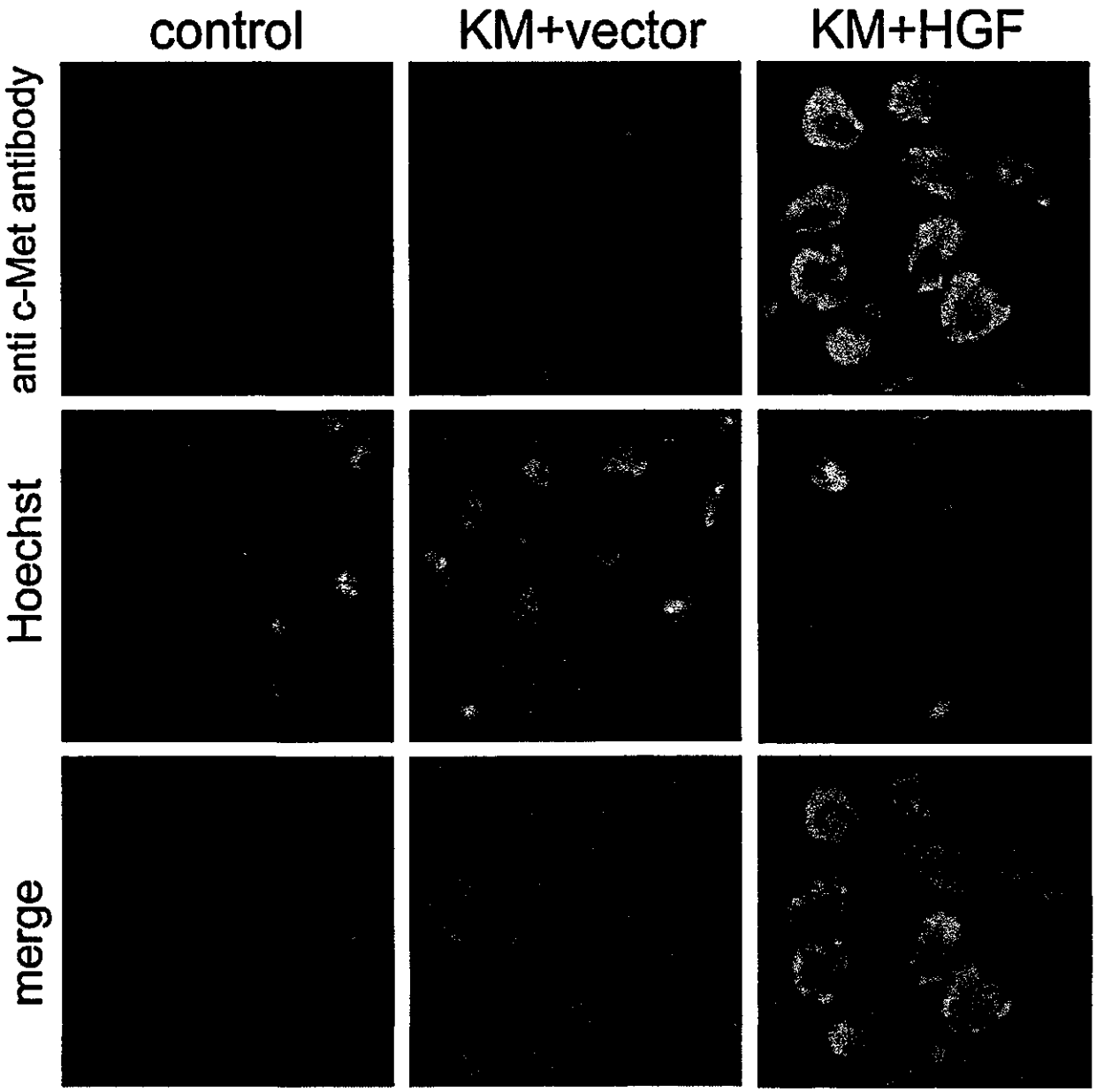

Figure 3. Enhancement of c-Met expression in SGCs by *HGF* gene transfer. Immunohistochemistry of SGCs from the intact rats, KM + vector group, and KM + HGF group was performed. Samples were stained with anti-c-Met antibody (upper) and counterstained with Hoechst 33342 (middle). Merged images are also presented (bottom).

Fig. 4

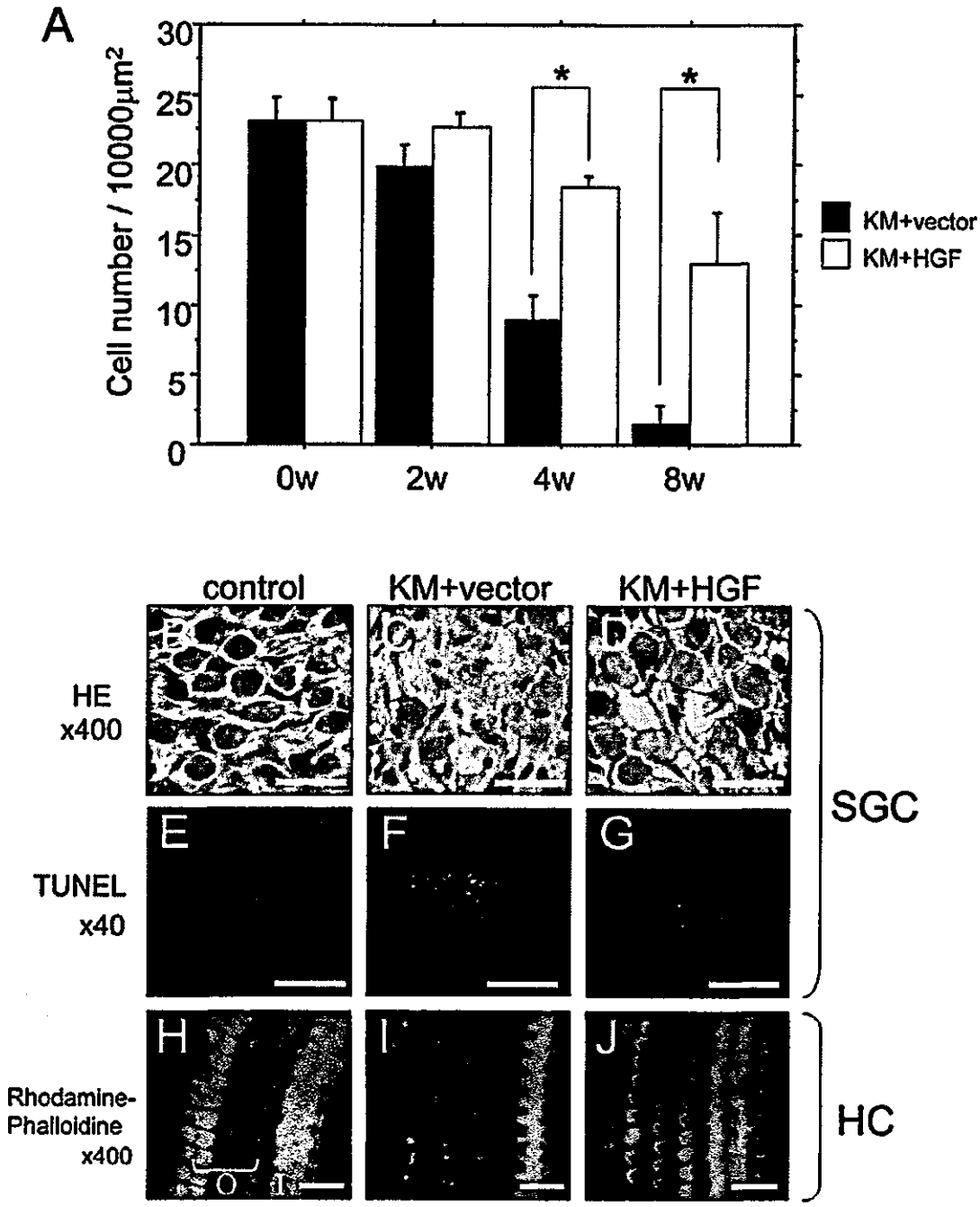

Figure 4. Protective effect of the HGF transgene on SGC and HC treated with kanamycin. Numbers of hematoxylin-positive cells of SGC of the rats treated with KM + vector or KM + HGF are counted at various time points (*A*; n=6 for each group). Mid-modiolar 10 μm cryosections from rats without treatment (control; *B*), treated with kanamycin and HVJ-E containing control vector (*C*), or HVJ-E containing the human HGF gene (*D*) were stained with hematoxylin on week 4. TUNEL staining of the contiguous sections of SGCs from the same rats as described above is shown in *E*, *F*, and *G*. Fluorescent image of HC of the rats in the control, KM + vector group, and KM + HGF group is shown in *H*, *I*, and *J*. O: outer hair cell; I: inner hair cell. Scale bar: 50 μm in *B-D* and *H-J*, 500 μm in *E-G*. *$P < 0.01$.

Fig. 5

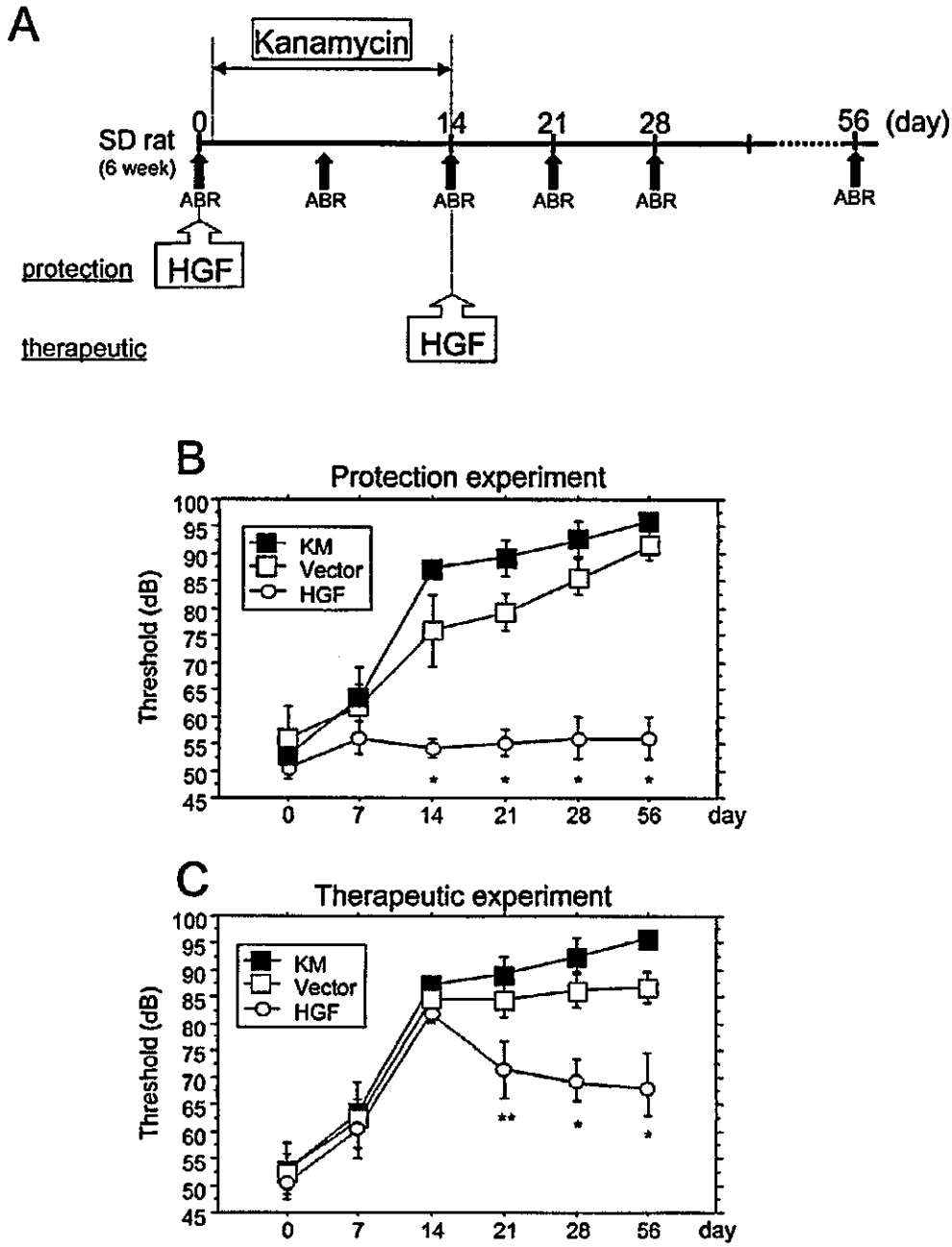

Figure 5. Hearing function of rats treated with KM, KM + vector, or KM + HGF was evaluated by the auditory threshold using ABR. Time course of the experiment was illustrated in *A*. In the protection experiment (*B*), rats treated with the HVJ-E containing control vector (vector) or HVJ-E containing the human *HGF* gene (HGF) immediately before the kanamycin insult underwent evaluation of the auditory threshold on days 0, 7, 14, 21, 28, and 56. In the therapeutic experiment (*C*), rats were treated with the HVJ-E containing control vector (vector) or HVJ-E containing the human *HGF* gene (HGF) 14 days after the kanamycin insult and the auditory threshold was measured at each time point. KM means the auditory threshold of rats treated only with kanamycin. Six rats were used in each group. Means ± SD of each value are indicated. ■: KM group; □: KM + vector group; ○: KM + HGF group. $^{*}P < 0.01$; $^{**}P < 0.05$.

Photodynamic therapy may be useful in debulking cutaneous lymphoma prior to radiotherapy

N. Umegaki, R. Moritsugu, S. Katoh, K. Harada, H. Nakano, K. Tamai, K. Hanada and M. Tanaka*

*Departments of Dermatology and *Pathology, Hirosaki University School of Medicine, Japan*

Summary

Photodynamic therapy (PDT) with topical 5-aminolaevulinic acid (5-ALA) is a promising new treatment for superficial malignant nonmelanoma tumours, including cutaneous malignant lymphoma. Here, we report a case of cutaneous anaplastic large cell lymphoma effectively treated by PDT with topical 5-ALA in combination with radiotherapy.

Report

Photodynamic therapy (PDT) has been shown to be a new and effective treatment for various cutaneous malignancies such as Bowen's disease, actinic keratosis, basal cell carcinoma and squamous cell carcinoma.[1] Recently, performance of PDT with topical 5-aminolaevulinic acid (5-ALA) for mycosis fungoides and CTCL has been reported with favourable clinical results.[2–4] In the present paper, we report the successful use of PDT with 5-ALA in a patient with cutaneous anaplastic large cell lymphoma (ALCL), one subset of malignant lymphoma.

A 69-year-old Japanese female with an unremarkable medical history developed an asymptomatic, enlarging skin tumour on the scalp; at the time of presentation this had been present for the 3 months. Physical examination revealed a 22 × 30-mm dome-shaped, reddish-violet tumour on the vertex of the scalp (Fig. 1). The lesion was covered with shiny, thinned skin without ulceration and was attached to the subcutaneous structure. Careful palpitation failed to demonstrate significant regional lymphadenopathy. Biopsy showed a sheet of dense infiltrate from the superficial dermis to the deep dermis consisting of large atypical lymphoid cells with a large number of mitotic figures. The covering epidermis showed slight spongiosis associated with a thinned cornified layer (Fig. 2). Immunohistochemistry demonstrated that the cells were CD30 positive and CD3, CD79, CD15, S-100, HMB-45 and anaplastic lymphoma kinase protein negative. Southern blotting revealed clonal rearrangements in the T-cell receptor α, and γ genes, and the partial loss of β and δ genes was observed. Epstein–Barr virus and human T-cell leukaemia virus type 1 were not detected in the serum or biopsy specimen. Computed tomography failed to detect internal lymphadenopathy, as well as metastatic lesion. Based on these findings, a diagnosis of cutaneous ALCL was made. Tumour, node, metastases (TNM) classification was evaluated as T1, N0, M0, placing this lesion into stage IA in the staging classification of CTCL.[5] It was desirable to reduce the tumour volume as much as possible prior to the initiation of radiation therapy. Towards this end, informed consent was obtained for PDT with application of topical 5-ALA to the cutaneous ALCL tumour.

For photosensitization, 20% 5-ALA (Sigma) in Dortin (Chemofux, Vienna, Austria) – an oil-in-water emulsion – was applied to the tumour with no preparation before ALA application, and kept in place under an occlusive dressing for 6 h prior to illumination with visible light. The tumour area was irradiated with by a SUS66 illuminator (Ushio, Tokyo, Japan), a metal halide-lamp with emission spectra of 630 nm and 700 nm. At a fluence rate of 100 mW cm^{-2}, the lesion received 120 J/cm^2 (irradiation time 20 min).

To examine the mechanism of cell death induced by ALA-based PDT, sections obtained from the tumour

Correspondence: H. Nakano, Department of Dermatology, Hirosaki University School of Medicine, 5 Zaifu-cho, Hirosaki, 036-8562, Japan. Tel.: +81 172 39 5087. Fax: +81 172 37 6060.
E-mail: hnakano@cc.hirosaki-u.ac.jp

Accepted for publication 24 June 2003

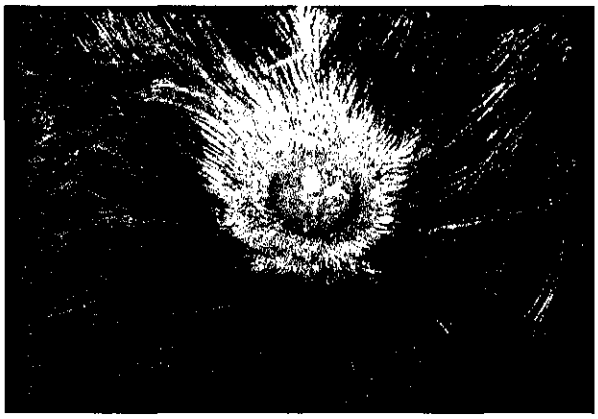

Figure 1 A dome-shaped, red tumour on the scalp.

Figure 2 Histology of the tumour prior to PDT demonstrates a dense infiltrate of large atypical lymphoid cells in the dermis. The covering epidermis shows slight spongiosis associated with a thinned cornified layer (haematoxylin & eosin, original magnification × 200).

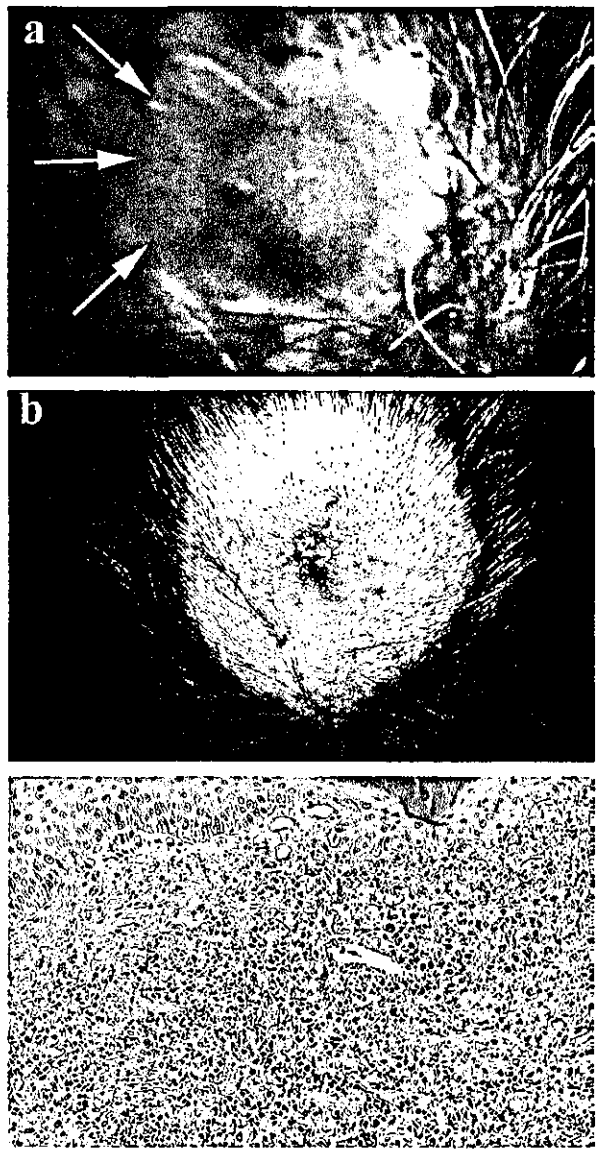

Figure 3 (a) The intense fluorescence of protoporphyrin IX was observed within the tumour. The peripheral region was also positive with a reduced intensity (arrows). (b) After the PDT sessions, the tumour mass became nearly flat, leaving residual infiltration. (c) Histology 24 h after the initial PDT showing massive degeneration of lymphoma cells, represented by numerous pyknotic nuclei (haematoxylin & eosin, original magnification × 200).

24 h after the initial PDT were examined for evidence of apoptosis, utilizing the terminal deoxynucleotidyl transferase-mediated *in situ* TUNEL method (*In situ* Apoptosis Detection Kit, Takara, Tokyo, Japan).

After removal of the 5-ALA ointment, a localized intense fluorescence was observed within the tumour under a Wood's light in a darkened room (Fig. 3a). The border of the tumour was also positive for fluorescence, albeit with a reduced intensity (Fig. 3a, arrows). The positivity, however, might not represent tumour specificity, because we did not confirm whether protoporphyrin IX was localized in the tumour cells or in the covering epidermis. After 9 consecutive days of treatment (total dose of 1080 J/cm^2), the tumour was remarkably reduced in volume and became almost flat. During treatment, the patient complained of a stinging sensation that was restricted to the illuminated area. Inflamed infiltration associated with moderate but tolerable pain remained at the tumour site and in the peripheral region of the initial tumour (Fig. 3b). Histology revealed massive degeneration of lymphoma cells, represented by numerous pyknotic nuclei, 24 h following the initial PDT (Fig. 3c). The remaining lesion underwent radiation therapy (total dose 40 Gy), and a

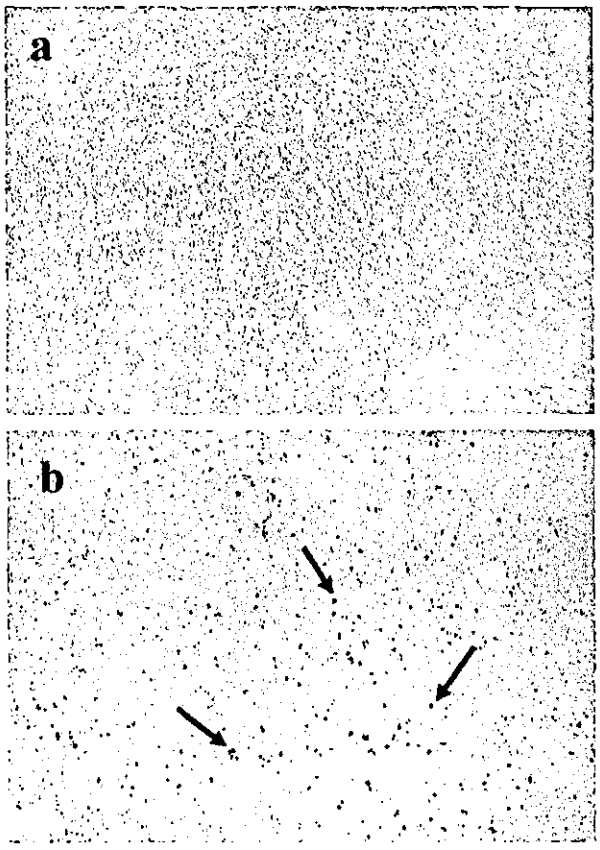

Figure 4 Apoptotic cells were detected by TUNEL using the *In Situ* Apoptosis Detection Kit (Takara, Tokyo, Japan) following the manufacturer's protocol. (a) Twenty-four hours after the initial PDT, few apoptotic cells are observed in a sheet of necrotizing lymphoma cells. Nuclei were counterstained by haematoxylin (original magnification × 100). (b) A significant number of apoptotic cells (arrows) are seen prior to PDT (original magnification × 100).

clinically disease-free condition resulted. The patient has not developed local recurrence for approximately 2 years.

In the immunohistochemical examination of apoptotic cells, virtually no apoptotic cells were detected throughout the dense collection of lymphoma cells undergoing necrosis 24 h after the initial PDT (Fig. 4a). In contrast, a significant number of apoptotic cells were observed in a sheet of atypical lymphoma cell infiltrate before PDT (Fig. 4b, arrows).

The lesion of cutaneous ALCL usually presents as a solitary, asymptomatic, cutaneous or subcutaneous reddish-violet tumour. ALCL accounts for approximately 9% of cutaneous lymphomas. Treatment of localized lesions usually includes excision with or without radiation and is associated with long-term survival.[5,6] As the present case was classified as stage IA with a localized cutaneous lesion, we chose PDT for the initial treatment to reduce the tumour volume before initiating ionizing radiation therapy. After nine consecutive PDT, the tumour mass was remarkably reduced, leaving an erythematous plaque with slight but discernible infiltration (Fig. 3b).

Generally, apoptosis is known to be one of the key mechanisms underlying the efficacy of PDT, while another mode of cell death, e.g. necrosis or vascular endothelial damage, might be involved in the cytotoxic mechanism.[7,8] Additionally, experimental reports demonstrated that the mode of cell death was dependent on the cell line, the photosensitizing agent and the protocol used.[9,10] These findings suggest that the mechanisms leading to cell death are complicated and difficult to assess. In order to address this, we performed immunohistochemical detection of apoptotic cells, using the terminal deoxynucleotidyl transferase-mediated *in situ* TUNEL method. Low numbers of apoptotic cells were observed throughout the dense infiltration of lymphoma cells undergoing necrosis 24 h after the first treatment of the PDT sessions (Fig. 4a). It is known that apoptotic cells can be spontaneously observed in CD30-positive ALCL, accounting for self-regression in some cases.[11] Indeed, we detected a significant number of apoptotic cells in a biopsy specimen obtained prior to PDT (Fig. 4b). In this case, we speculate that necrotic cell death may be the predominant mode of cytotoxicity elicited by PDT with topical ALA, although we could not exclude the possible involvement of apoptotic cell death, which might have been overwhelmed by the intensive necrosis.

Finally, in the present case PDT with topical 5-ALA in combination with radiotherapy was demonstrated to be an effective treatment for a localized lesion of cutaneous ALCL. Such PDT reduced the tumour volume prior to conventional therapy, and may contribute to minimizing the possible adverse effects by ionizing radiation and chemotherapy.

References

1 Kalka K, Merk H, Mukhtar H. Photodynamic therapy in dermatology. *J Am Acad Dermatol* 2000; **42**: 389–413.
2 Wolf P, Fink-Puches R, Cerroni L, Kerl H. Photodynamic therapy for mycosis fungoides after topical photosensitization with 5-aminolevulinic acid. *J Am Acad Dermatol* 1994; **31**: 678–80.
3 Markham T, Sheahan K, Collins P. Topical 5-aminoleavulinic acid photodynamic therapy for tumour-stage mycosis fungoides. *Br J Dermatol* 2001; **144**: 1262–3.

4 Edström DW, Porwit A, Ross A. Photodynamic therapy with topical 5-aminolevulinic acid for mycosis fungoides: Clinical and histological response. *Acta Derm Venereol* 2001; **81**: 184–8.
5 Fung MA, Murphy MJ, Hoss DM, Grant-Kels JM. Practical evaluation and management of cutaneous lymphoma. *J Am Acad Dermatol* 2002; **46**: 325–57.
6 Stein H, Foss HD, Dürkop H *et al.* CD30+ anaplastic large cell lymphoma: a review of its histopathologic, genetic, and clinical features. *Blood* 2000; **96**: 3681–95.
7 Hampton JA, Selman SH. Mechanism of cell killing in photodynamic therapy using a novel in vivo drug/in vitro light culture system. *Photochem Photobiol* 1992; **56**: 235–43.
8 Gibson SL, van der Meid KR, Murant RS, Hilf R. Increased efficacy of photodynamic therapy of R3230AC mammary adenocarcinoma by intratumoural injection of photofrin II. *Br J Cancer* 1990; **61**: 553–7.
9 He X-Y, Sikes R, Thomsen S *et al.* Photodynamic therapy with photofrin II induces programmed cell death in carcinoma cell lines. *Photochem Photobiol* 1994; **59**: 468–73.
10 Dellinger M. Apoptosis or necrosis following Photofrin photosensitization: influence of the incubation protocol. *Photochem Photobiol* 1996; **64**: 182–7.
11 Levi E, Wang Z, Petrogiannis-Haliotis T *et al.* Distinct effects of CD30 and Fas signaling in cutaneous anaplastic lymphomas: a possible mechanism for disease progression. *J Invest Dermatol* 2000; **115**: 1034–40.

Experimental Dermatology 2004: 13: 773–779
Blackwell Munksgaard . Printed in Denmark

EXPERIMENTAL DERMATOLOGY
ISSN 0906-6705

Transcriptional regulation of the 230-kDa bullous pemphigoid antigen gene expression by interferon regulatory factor 1 and interferon regulatory factor 2 in normal human epidermal keratinocytes

Odanagi M, Kikuchi Y, Yamazaki T, Kaneko T, Nakano H, Tamai K, Hanada K. Transcriptional regulation of the 230-kDa bullous pemphigoid antigen gene expression by interferon regulatory factor 1 and interferon regulatory factor 2 in normal human epidermal keratinocytes. Exp Dermatol 2004: 13: 773–779. © Blackwell Munksgaard, 2004

Abstract: Interferon regulatory factors (IRFs) are a family of transcriptional factors induced by interferon-γ (IFN-γ). Recent studies have indicated that the deregulation of IRF system in keratinocytes is responsible, at least in part, for aberrant proliferation and the differentiation of the psoriatic epidermis. Previously, we reported that the expression of 230-kDa bullous pemphigoid antigen (*BPAG1*) gene, which is strictly restricted to basal keratinocytes, is transcriptionally suppressed by IFN-γ, but the contribution of IRFs in such suppression is still unclear. In this study, we investigated the role of IRFs in the regulation of BPAG1 gene expression. Computer analysis identified IRF1 and IRF2 consensus sequences between −135 and −123 on BPAG1 promoter region. Transient transfection studies with BPAG1 promoter-luciferase reporter gene plasmids and IRF1 and IRF2 expression plasmids revealed that IRF1 and IRF2 directly down-regulated BPAG1 gene transcription in cultured normal human epidermal keratinocytes. Several sets of gel retardation assays with the BPAG1–IRF binding sequence as a probe indicated that IRF1 and IRF2 could bind to the BPAG1–IRF sequence, but some other protein(s), which was induced by IFN-γ stimulation and possessed binding activity to IRF consensus sequence, showed preferential binding to the BPAG1–IRF sequence. Our results suggest that IFN-γ–IRF system is involved in BPAG1 gene regulation in type-1 helper T-cell inflammatory skin conditions, such as psoriasis vulgaris.

Maiko Odanagi[1], Yasushi Kikuchi[1], Takehiko Yamazaki[1], Takahide Kaneko[1], Hajime Nakano[1], Katsuto Tamai[2], Joani Vitto[3] and Katsumi Hanada[1]

[1]Department of Dermatology, Hirosaki University School of Medicine, Aomori, Japan; [2]Division of Gene Therapy Science and Department of Dermatology, Osaka University Graduate School of Medicine, Osaka, Japan; [3]Department of Dermatology and Cutaneous Biology, Jefferson Medical College, Philadelphia, PA, USA.

Key words: differentiation – IFN-γ – IRF – psoriasis

Maiko Odanagi, MD
Department of Dermatology
Hirosaki University School of Medicine
5 Zaifu-cho
Hirosaki 036-8562
Japan
Tel.: +81 172 39 5087
Fax: +81 172 37 6060
e-mail: derma@cc.hirosaki-u.ac.jp

Accepted for publication 7 April 2004

Introduction

Interferon-γ (IFN-γ) is a multifunctional type-1 helper T (Th1)-cell cytokine, e.g. antiviral effects, regulation of Th1 type immune reaction, modulation of cell growth and differentiation (1,2). On epidermal keratinocytes, IFN-γ has been shown to induce the expression of intercellular adhesion molecule-1 (ICAM-1) and antihuman leukocyte antigen-DR (HLA-DR) (3,4) and inhibit proliferation and induce aberrant differentiation (5).

IFN-γ-mediated gene regulation is initiated by IFN-γ binding to the cell-surface receptor, followed by the induction of the activation of adjacent Janus kinase (JAK) 1 and 2 to phosphorylate tyrosine residues of signal transducer and activator of transcription (STAT1). This kinase reaction, so called JAK-STAT signal transduction system, results in homo dimmer formation of STAT1 protein, followed by nuclear translocation and binding to gamma interferon activation site (GAS) residing in the regulatory region of the target genes (6,7). The interferon regulatory factors (IRF) family is a set of transcriptional factors regulated by JAK-STAT signal transduction system, and at present, nine IRF members (IRF1 to

IRF9) have been identified in various cell types and tissues (8). Expression of IRF1 has been noted in almost all cell types, including epidermal keratinocytes, and is involved in the transcription of IFN-α, IFN-β and antiviral activity of IFN-α, IFN-β, and IFN-γ (9). IRF1 has been shown to function as anti-oncogenic factor and to play an important role in the regulation of apoptosis and cell-cycle arrest (10,11). IRF2 is another major member of this family identified in various cell types. IRF2 shows 62% homology to IRF1 at mRNA sequence level, and both factors bind to the same DNA motif on the target DNA regulatory region (9,12). In general, compared with IRF1, IRF2 tends to show a relatively weak response to IFN-γ and to play adverse roles such as oncogenic activity based on the rapid acceleration of cell growth (10,13). These observations suggest that imbalance of IRF1 and IRF2 may be involved in aberrant growth and differentiation of various IFN-related inflammatory diseases including psoriasis vulgaris, which exhibits disorganized epidermal differentiation and proliferation. This hypothesis is further supported by the reports that psoriasiform inflammatory skin lesions were induced on the IRF2 knockout mouse (14,15) and that disorganized response to IRF1 was observed in cultured keratinocytes from psoriatic epidermis (16).

The epidermis is a multilayered squamous epithelium composed of a basal layer of proliferating and undifferentiated keratinocytes, spinous layers of differentiated keratinocytes, granular layers of preapoptotic keratinocytes, and horny layer of apoptotic keratinocytes acting as an epidermal barrier. IFN-γ is known to induce aberrant keratinocyte differentiation *in vitro* and *in vivo* (17,18). We have also investigated IFN-γ-dependent regulatory mechanisms of the epidermal genes including the 230-kDa bullous pemphigoid antigen (*BPAG1*) (19), which is specifically expressed in the undifferentiated basal keratinocytes as a component of the hemidesmosome securing those keratinocytes to the underlying basement membrane (20). We have recently identified a novel interferon gamma inhibitory element (IGIE), which is responsible for IFN-γ-dependent transcriptional down-regulation of the *BPAG1* gene, in the region between −80 and −60 from the transcription starting site (17) (Kaneko et al. unpublished data). IGIE contains chimera sequences composed of partial sequences of interferon stimulating responsive element (ISRE) and GAS, both of which are well characterized as *cis*-elements targeted by JAK-STAT signal transduction. Mutagenesis of IGIE sequence, however, failed to completely disturb the IFN-γ-dependent down-regulation of *BPAG1* gene (Kaneko et al. unpublished data), suggesting the existence of an additional regulatory mechanism(s) besides IGIE system. In this study, we examined the role of the IRF regulatory system on the IFN-γ-dependent BPAG1 down-regulation to elucidate the molecular mechanisms involved in aberrant epidermal differentiation induced by IFN-γ.

Materials and methods

Cell culture

Normal human epidermal keratinocytes (NHEKs) were cultured in keratinocyte growth medium (KGM) containing epidermal growth factor, bovine pituitary extract, insulin, and hydrocortisone (Clontech Corp., San Diego, CA, USA) at 37°C under 5% CO_2 and 95% air. The cell cultures were treated by trypsinization and studied at passage 3.

RNA isolation and Northern blot analysis

Total cellular RNAs were isolated from NHEK, which were either unstimulated or stimulated by IFN-γ(100 U/ml) for 10, 30 min, 1, 3, 6, 12, 24, or 48 h, and the other order by IFN-γ 10, 100, 1000 U/ml for 24 h, using the RNeasy Mini Kit (Qiagen, Hilden, Germany). The isolated RNAs (20 μg/lane) were electrophoresed in a 1% agarose gel containing 18% formaldehyde and transferred to a Hybond N membrane (Amersham, Aylesbury, UK). The membrane was prehybridized and then hybridized with a 400-bp human IRF1 or IRF2 cDNA from 501 to 900 (in relation to the transcription initiation site) as a probe. These probes were obtained by using Prime-It® RmT Random Primer Labeling Kit (Stratagene, La Jolla, CA, USA) and radioactively labeled with [α-^{32}P]dCTP (NEN® Life Science Products, Inc., Boston, MA). After hybridization (24 h at 43°C), the membranes were washed with 2 × saline sodium citrate (SSC) in 0.1% sodium dodecyl sulfate (SDS) for 20 min at room temperature and 1 × SSC in 0.1% SDS for 10 min at 42°C. The membranes were then exposed to X-ray films (Fuji Film, Tokyo, Japan). The IRF1 and IRF2 mRNA levels were normalized to glyceraldehyde 3-phosphate dehydrogenase (G3PDH) mRNA transcripts in the same RNA preparations. Blots were scanned and the intensity of each band was measured by computer software program NIH image.

Plasmid construction cDNAs of IRF1 and IRF2 were obtained by reverse transcription-polymerase chain reaction (RT-PCR). The reverse transcriptase reaction was carried out with 2 μg total RNA isolated from NHEK for first strand cDNA. The primers of the human *IRF1* gene used in this study were the sense primer for PCR, 5′-GGGAAGCTTC-GAATCGCTCCTGCAGCAGA-3′ and the antisense primer 5′-CCCGAATTCCTTGCCTAGAGGAATAAGAG-3′. The primers of the human *IRF2* gene were the sense primer, 5′-GGGAAGCTTTGCGGAATTGTATTGGTAGC-3′ and the antisense primer, 5′-CCCAAGCTTGAGAGTCAGAGGCT-TAACAG-3′. The obtained fragments of *IRF1* (1039-bp) and *IRF2* (1109-bp) were each ligated into the *Hind*III/*Eco*R1 and *Hind*III/*Hind*III sites of pCY4B expression vector. Then, IRF1 or IRF2 and pCY4B were ligated at 5:1 ratio of concentration using DNA Ligation kit (Ver. 2, Takara, Tokyo, Japan) at 15°C, overnight. These expression vectors of IRF1 and IRF2 were verified by sequencing. The 5′-deletion constructs, designated as pBP146luc, pBP88luc, and pBP59luc, which included −146/+101, −88/+101, and −59/+101 of BPAG1 promoters, respectively, were linked to the luciferase reporter gene vector pGL3-luc (Promega, Madison, WI, USA).

Transient transfection and luciferase assay

Transfection of plasmid DNA into NHEK was performed by Lipofectamine (Invitrogen, San Diego, CA, USA). The promoter/luciferase construct (2 μg) was used in transient transfection of NHEK (6-cm diameter culture dish) cultured in KGM with 2 μg each of IRF1 and IRF2 expression vectors or pCY4B. Twenty-four hours after transfection, cells were washed twice in phosphate-buffered saline (PBS), dissolved in 400 μl Reporter Lysis Buffer (Promega), and harvested by scraping. Luciferase assay was performed by using Luciferase Assay System (Promega) and luminometer Lumat LB9501 (Berthold, Bad Wildbad, Germany). pSV-β-galactosidase was co-transfected in every experiment, and the β-galactosidase activities were measured by fluorescence intensity using luminometer LB9501 and used to monitor the transfection efficiency. All experiments were performed in triplicate.

Nuclear extracts

NHEK cultures were stimulated by IFN-γ(100 U/ml) for 0, 1, 3, 6, 12, or 24 h. Nuclear extracts were obtained as described previously (16).

Electrophoretic mobility shift assays (EMSAs)

We used two oligonucleotides as probes. One was named BPAG1-IRF (5'-AATACAAGCTAC AAAAGGCAAACCT-CAGCTAGC A-3'), which contained a binding site for IRF in BPAG1 promoter. The other was named consensus-IRF (5'-AAGTGAAAGTGAAAGTGA-3'), which contained the consensus-binding site for IRF. Oligos were annealed before labeling by heating to 98°C for 10 min and cooling slowly to room temperature. Double-stranded oligos (10 pmol) were end-labeled with [γ-^{32}P]dATP (NEN™ Life Science Products Inc.) using T4 polynucleotide kinase (Takara) and purified using Sephadex G-25 spin columns (Roche Molecular Biochemicals, Mannheim, Germany), followed by measurement of the radiation dose. Binding reactions were carried out by incubation on ice for 30 min. Binding reactions were treated with 5 μg of nuclear extract, 8 μl of 2.5 × buffer, 0.5 mM dithiothreitol (DTT), 2 μl of polyd (I-C) (1 μg/ml) (Roche Molecular Biochemicals), and 60000 cpm-labeled DNA in 20 μl binding reactions. Competition experiments were carried out by adding unlabeled oligo to the binding reactions before the addition of the labeled probe. Supershift experiments to confirm the identity of the bound protein were performed by the addition of 1 μg of the specific antibodies to either IRF1 or IRF2 (Santa Cruz, Autogen Bioclear UK, Wilts, UK) to the binding reactions. After the addition of antibodies, binding reactions were incubated on ice for 30 min before separating DNA-protein complexes on 8% polyacrylamide at 200 V for 3 h. Gels were fixed in 10% acetic acid and 30% methanol before vacuum drying and exposure to autoradiographic film (Fuji Film).

Results

Induction of IRF1 and IRF2 mRNAs expression by IFN-γ in NHEK

Subconfluent cultures of NHEK were incubated with 0, 10, 100, or 1000 U/ml of IFN-γ for 24 h, then total RNAs were isolated and subjected to Northern blot analyses for IRF1, IRF2, and G3PDH mRNA expression. No IRF1 expression was observed without IFN-γ stimulation, but strong and maximum induction of IRF1 mRNA expression was noted by treatment with 100 U/ml of IFN-γ. Less, but significant, IRF1 mRNA expression was induced by 1000 U/ml of IFN-γ (Fig. 1a). In contrast, IRF2 mRNA expression was obvious in cultured NHEK without IFN-γ treatment. A similar mRNA induction pattern as IRF1 was also observed for IRF2, and treatment of NHEK with 100 U/ml of IFN-γ yielded maximum induction (Fig. 1a). Time-dependent inductions of both IRF1 and IRF2 mRNA expression were also observed by Northern blot analysis of NHEK cultures treated with 100 U/ml of IFN-γ for various incubation periods, and strong induction was observed already after 3-h incubation (Fig. 1b). Even after 48-h incubation, significant increases of IRF1 and IRF2 mRNA expression were still noted in these cultures (Fig. 1b). In both dose- and time-dependent experiments, IRF1 induction exhibited a higher sensitivity to IFN-γ treatment compared to IRF2. In fact, only 2- to 3-fold increase of IRF2 expression was noted in these experiments, while more than 10-fold increase in IRF1 expression occurred. The IRF1 and IRF2 mRNA levels were expressed relative to those of G3PDH mRNA transcripts in the same RNA preparations.

Computer search for IRF binding consensus sequence in the BPAG1 promoter region

As IFN-γ transcriptionally down-regulates BPAG1 expression, IRF binding consensus sequence was explored in the BPAG1 promoter region by computer search program. A putative IRF binding site was identified in the region between −135 to −123 from transcription starting site, and designated as BPAG1–IRF, which had a homology in 10 of 13 bases of consensus IRF sequence (Fig. 2). BPAG1–IRF is located 43 bases upstream from IGIE, which is responsible in part for down-regulation of BPAG1 by IFN-γ (Kaneko et al. unpublished data).

Deletion analysis to explore function of BPAG1–IRF site in the promoter

To examine whether IRF1 and IRF2 function to regulate BPAG1 promoter activity through BPAG1–IRF site, human IRF1 and IRF2 expression plasmid vectors and three different deletion constructs of the BPAG1 promoter-luciferase reporter gene plasmids, pBP146luc, pBP88luc, and pBP59luc, were generated. Transient transfection studies were performed by co-transfection of either IRF1 or IRF2 expression vector, or mock plasmid pCY4B, with one of these deletion promoter-luciferase gene constructs in NHEK cultures. Both IRF1 and IRF2 expression vectors, but not mock plasmid, down-regulated the promoter activity of pBP146luc plasmid (Fig. 3). However, similar transfection studies with pBP88luc, in

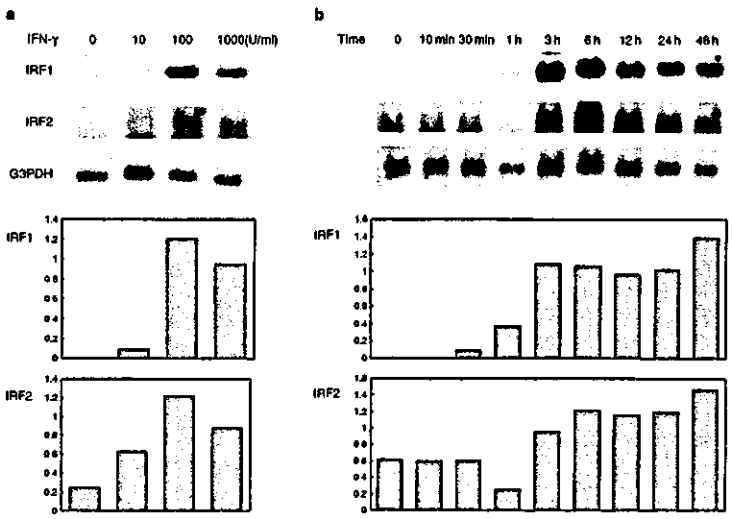

Figure 1. a) Interferon regulatory factors IRF1 and IRF2 mRNA expression levels in normal human epidermal keratinocyte (NHEK) cells are dependent on interferon-γ (IFN-γ) dose. Cultures of NHEK cells (at 80% confluence) were treated with 0, 10, 100, or 1000 U/ml of IFN-γ and total RNAs were isolated after incubation for 24 h, and northern blot analyses with IRF1, IRF2 and glyceraldehyde-3-phosphate dehydrogenase (G3PDH) were performed. The expression of IRF1 and IRF2 mRNAs reached maximal levels in cultures treated with 100 U/ml of IFN-γ. IFN-γ-untreated NHEK cells showed no IRF1 mRNA expression and a slight expression of IRF2 mRNA. (b) Serial changes in IRF1 and IRF2 mRNA expression levels in NHEKs treated with 100 U/ml of IFN-γ. The expression of IRF1 mRNA showed strong induction after 3 h incubation. IRF2 mRNA expression increased with time after IFN-γ stimulation. The IRF1 and IRF2 mRNA expression levels were normalized by G3PDH mRNA transcripts in the same RNA preparations.

which BPAG1–IRF site was deleted, resulted in failure of down-regulation by IRF1 and IRF2, in addition to more than 50% reduction of the basal promoter activity. Further deletion of both BPAG1–IRF site and IGIE sequence in pBP59luc basically provided similar results by IRF1 and IRF2 expression as shown by pBP146luc. Further reduction of the basal promoter activity was observed following IGIE deletion, although it was not statistically significant.

Identification of BPAG1–IRF binding protein by electrophoretic mobility shift assay

To identify and characterize BPAG1–IRF binding proteins in NHEK, we performed EMSA using NHEK nuclear extracts. First, we evaluated the binding activities of consensus–IRF sequence to the extracts. Radiolabeled consensus–IRF oligo-DNA was incubated with nuclear extracts from cultured NHEK that had been treated with 100 U/ml of IFN-γ for various incubation periods and subjected to EMSA. In the nuclear extracts, at least two different binding activities (bands a and d) were induced by IFN-γ after 3-h incubation, and the expression of these shifted complex was persistently noted even at 24 h (Fig. 4a). Other two strong binding (bands b and c) were also observed, and enhanced binding activity of band b was

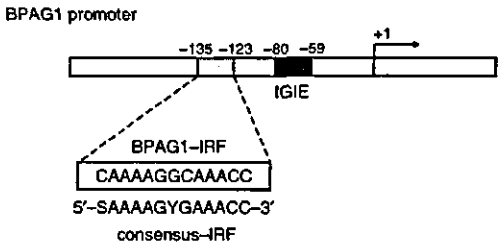

Figure 2. Schematic representation of the 230-kDa bullous pemphigoid antigen (BPAG1) promoter. The BPAG1 promoter contains the elements of BPAG1–interferon regulatory factor (IRF) and interferon gamma inhibitory element (IGIE). We named IRF–consensus element within BPAG1 promoter as BPAG1–IRF. BPAG1–IRF element exists from −135 to −123 of BPAG1 promoter relative to the transcriptional start site. We named chimeric element of interferon stimulating responsive element (ISRE), consensus, and gamma interferon activation site (GAS) elements within BPAG1 promoter as IGIE. IGIE exists from −80 to −59 of BPAG1 promoter.

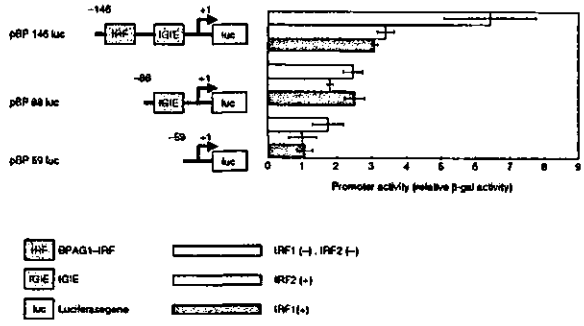

Figure 3. Deletion analyses for interferon regulatory factor (IRF) responsive element in 230-kDa bullous pemphigoid antigen (BPAG1) promoter. The structures of the BPAG1 promoter in the reporter plasmids are depicted on the left. The BPAG1 promoter deletion, pBP146luc contains IRF1, IRF2, and interferon gamma inhibitory element (IGIE)-responsive element, pBP88luc contains IGIE-responsive element while pBP59 luciferase lacks IRF1, IRF2, and IGIE. Each construct was transfected in the presence of IRF1 and IRF2 expression vector or pCY4B, and then the promoter activity was measured as luciferase activity. Luciferase activities were expressed relative to β-galactosidase activity. In the presence of IRF1, pBP146luc showed 50% less luciferase activity than in the absence of IRF1.